Dynamic Characterization of Frequency Response of Shock Mitigation of a Polymethylene Diisocyanate (PMDI) Based Rigid Polyurethane Foam

Bo Song<sup>1</sup>, Kevin Nelson<sup>2</sup>

<sup>1</sup> Sandia National Laboratories, Albuquerque, NM 87185, USA

<sup>2</sup> Sandia National Laboratories, Livermore, CA 94551, USA

### **Abstract**

Kolsky compression bar experiments were conducted to characterize the shock mitigation response of a polymethylene diisocyanate (PMDI) based rigid polyurethane foam, abbreviated as PMDI foam in this study. The Kolsky bar experimental data was analyzed in the frequency domain with respect to impact energy dissipation and acceleration attenuation to perform a shock mitigation assessment on the foam material. The foam specimen thickness and applied impact speed were varied, in order to investigate these effects on the frequency response related to the amount of impact energy dissipation and acceleration attenuation through the foam samples. The PMDI foam material exhibits excellent performance in both energy dissipation and acceleration attenuation, particularly for the impact frequency content over 1.5 kHz. This frequency (1.5 kHz) was observed to be independent of specimen thickness and impact speed, which may represent the characteristic shock mitigation frequency of the PMDI foam material under investigation.

The shock mitigation characteristics of the PMDI foam material, consisting of the energy dissipation ratio and acceleration attenuation, were insignificantly influenced by the specimen thickness. However, impact speed did have some effect.

# Keywords

Kolsky compression bar, foam material, shock mitigation, frequency response, energy dissipation, acceleration

#### Introduction

Polymeric foams have been widely used as shock mitigation materials in many applications that include transportation vehicles, electronic packaging, hazardous material storage and transportation, and head protection, etc. The main purpose of using foam materials is to prevent critical electronic and magnetic assemblies from mechanical failure, as well as, protect passengers from severe head injury when they are subjected to a variety of loading from low to high speed impact up to and including shock or blast loading [1-5]. Such applications benefit from the unique lightweight and high impact energy absorption properties of foam materials. Important mechanical parameters, energy absorption and transmitted force/acceleration, acting through the foam materials have been identified to be critical to mitigate external shock or impact load. In applications, the foam materials need to be carefully designed, selected, and/or optimized to be capable of maximizing the amount of energy absorption with minimal transmitted force and acceleration. However, the shock mitigation performance of the foam materials depends on both the specific external loading condition and the criteria of internal components being protected. For example, the internal components may be sensitive to a specific range of frequency, which requires the foam materials to be designed to absorb the energy and acceleration effectively in this specific frequency range for better protective effectiveness and efficiency. In this case, it is desirable to understand the frequency sensitivities of the foam materials in terms of energy absorption and transmitted acceleration.

Currently, the shock mitigation of foam materials is evaluated with respect to the total amount of energy that can be absorbed [1, 6]. The calculation of energy absorption is usually based on the compressive stress-strain response of the foam materials. In the past years, many different foam materials have been experimentally characterized in terms of compressive stress-

strain response under different loading and environmental conditions that include various densities, strain rates, temperatures, and stress states [7-12]. Polymeric foam materials have been found to exhibit stress-strain responses with significant effects of strain rate, temperature, and stress state, which make their energy absorption also dependent on the temperature and loading conditions.

The acceleration transmitted through the foam materials has been investigated with impact or drop tests [5, 6]. Upon impact or drop loading, accelerometers were placed on the back side (opposite to the impact side) of the components to directly measure the transmitted acceleration. Both impact energy absorption and acceleration attenuation have been commonly investigated in the time domain, which limits the understanding of the frequency response of the foam materials in terms of impact energy absorption and acceleration attenuation.

In this study, we employed the Kolsky compression bar, also called split Hopkinson pressure bar (SHPB), to investigate the frequency response of impact energy absorption and acceleration attenuation of a polymethylene diisocyanate (PMDI) based rigid polyurethane foam, abbreviated as PMDI foam henceforth. PMDI foams have demonstrated excellent survivability for encapsulated devices from mechanical vibration or impact loading [13]. Since they are environmentally friendly, the PMDI foams have been more widely used as a structural component to mitigate mechanical shock. The compressive stress-strain response and its dependence on strain rate and temperature has been fully characterized [12]. However, the frequency domain characteristics of impact energy absorption and acceleration attenuation through the PMDI foams have not been fully understood yet.

The energy analyses in Kolsky bar experiments have been conducted in time domain [14, 15], while the frequency analysis in Kolsky bar experiments has been limited to stress wave dispersion correction [16, 17]. The purpose of this study was to analyze the impact energy and acceleration in the frequency domain in order to investigate the frequency spectra of absorbed impact energy and transmitted acceleration through the PMDI foam material. The PMDI foam specimens were varied in thickness and subjected to two different impact speeds to determine the effects of specimen thickness and impact speed on the frequency response of impact energy absorption and acceleration attenuation.

## **Dynamic Experiments and Frequency Domain Analysis**

The dynamic compressive experiments were conducted with a conventional Kolsky compression bar, the schematic of which is shown in Fig. 1. The compression bar system consists of a striker, an incident bar and a transmission bar with a common diameter of 19.05 mm. The striker and pressure bars were made of C350 maraging steel. Upon the impact of striker on the end of incident bar, a square-like pulse is generated and propagates toward the foam specimen that is sandwiched between the incident and transmission bars. It is noted that no pulse shaper has been employed in this study because a direct impact is preferable to generate an impact load with high-amplitude and high-frequency accelerations as an experimental simulation of mechanical shock environments. When the stress wave propagates to the specimen, part of the incident wave is reflected back and the remaining part of the wave transmits into the transmission bar through the specimen. The strain gages on the incident bar record the incident and reflected pulses while the strain gages on the transmission bar record the transmitted pulses.

In this study, we are looking at the structural response of the foam material instead of the material property characterization. The requirements of stress equilibrium and uniform deformation during dynamic loading are not necessarily satisfied. In addition, no lubricant has been applied to the bar/specimen interfaces in order to avoid the effect of lubricant on the frequency analysis.

After the incident, reflected, and transmitted pulses are recorded, the energies associated with all three pulses are calculated in the time domain with the following equations [14, 15],

$$E_i(t) = A_0 C_0 E_0 \int_0^t \varepsilon_i(t)^2 dt \tag{1}$$

$$E_r(t) = A_0 C_0 E_0 \int_0^t \varepsilon_r(t)^2 dt \tag{2}$$

$$E_{t}(t) = A_{0} C_{0} E_{0} \int_{0}^{t} \varepsilon_{t}(t)^{2} dt$$

$$\tag{3}$$

where the subscripts, i, r, and t represent incident, reflected, and transmitted strains, respectively;  $A_0$  is the cross-sectional area of the pressure bars;  $C_0$  and  $E_0$  are one-dimensional elastic wave speed and Young's modulus of the bar material. In general, Kolsky bar experiments have the incident and transmission bars made of the same material and with the same diameter. The energy dissipation through the specimen is thus calculated as

$$\Delta(t) = E_i(t) - E_r(t) - E_t(t) = A_0 C_0 E_0 \int_0^t \left[ \varepsilon_i(t)^2 - \varepsilon_r(t)^2 - \varepsilon_t(t)^2 \right] dt \tag{4}$$

The energy dissipation ratio,  $\delta(t)$ , is defined as the ratio of total energy dissipated to the total energy being input into the specimen,

$$\delta(t) = \frac{\Delta(t)}{E_i(t) - E_r(t)} = \frac{\int_0^t \left[\varepsilon_i(t)^2 - \varepsilon_r(t)^2 - \varepsilon_t(t)^2\right] dt}{\int_0^t \left[\varepsilon_i(t)^2 - \varepsilon_r(t)^2\right] dt}$$
(5)

In theory, the dissipated energy and energy dissipation ratio are time dependent. However, due to the wave dispersion, the bar strain histories measured at the strain-gage locations may not represent the actual strains at the bar/specimen interfaces [16, 17]. The histories of dissipated energy and associated energy dissipation ratio are not accurate until wave dispersion is properly corrected. However, the total amount of dissipated energy and energy dissipation ratio over the entire duration of loading may still be usable. In addition, the time domain analyses of dissipated energy and energy dissipation ratio do not provide any information on the dependence of frequency on the energy dissipation characteristic of the material under investigation. Instead, direct frequency domain analysis is needed to investigate the frequency response of shock mitigation in terms of impact energy dissipation through the foam material.

Consider a time domain bar strain signal,  $\varepsilon(t)$ , it has the following Fourier transform,

$$\varepsilon(f) = B(f)e^{-j(2\pi f + \phi)} \tag{6}$$

where B(f), f and  $\phi$  are magnitude, frequency and phase in the Fourier transform, respectively. The energy spectrum density, associated with the bar strain, in the frequency domain has a similar form as expressed with Eqs. (1)-(3) [18],

$$S(f) = A_0 C_0 E_0 |B(f)|^2 \tag{7}$$

Therefore, in a Kolsky bar experiment, the incident, reflected, and transmitted energy spectral densities can be expressed in frequency domain,

$$S_{i}(f) = A_{0}C_{0}E_{0}|B_{i}(f)|^{2}$$
(8)

$$S_r(f) = A_0 C_0 E_0 |B_r(f)|^2 \tag{9}$$

$$S_{t}(f) = A_{0}C_{0}E_{0}|B_{t}(f)|^{2}$$
(10)

where  $B_i(f)$ ,  $B_r(f)$ , and  $B_t(f)$  are the magnitudes of Fourier transforms on the incident, reflected, and transmitted bar strains, respectively. The energy spectrum density in the frequency domain represents the energy distribution over frequencies. The total energy at a specific frequency can be calculated as,

$$E(f) = \int_{f}^{f + \Delta f} S(f) df = A_0 C_0 E_0 \int_{f}^{f + \Delta f} |B(f)|^2 df \approx A_0 C_0 E_0 |B(f)|^2 \Delta f$$
 (11)

The energy dissipation in the specimen is

$$\Delta(f) = E_t(f) - E_t(f) - E_t(f) = A_0 C_0 E_0 (|B_t(f)|^2 - |B_t(f)|^2 - |B_t(f)|^2) \Delta f$$
(12)

and the energy dissipation ratio is computed with the following equation,

$$\delta(f) = \frac{\Delta(f)}{E_i(f) - E_r(f)} = 1 - \frac{|B_i(f)|^2}{|B_i(f)|^2 - |B_r(f)|^2}$$
(13)

Equation (13) represents how energy dissipation through the specimen is sensitive to frequencies.

Besides impact energy, acceleration is another parameter critical to the survivability of internal electronic or magnetic devices/components. The acceleration directly applied to the test sample is calculated as

$$a_{input}(t) = \frac{dV_{input}(t)}{dt} = C_0 \frac{d(\varepsilon_i(t) - \varepsilon_r(t))}{dt} = a_i(t) - a_r(t)$$
(14)

where  $a_i(t)$  and  $a_r(t)$  are acceleration histories represented by the incident and reflected pulses, respectively,

$$a_i(t) = C_0 \frac{d\varepsilon_i(t)}{dt} \tag{15}$$

$$a_r(t) = C_0 \frac{d\varepsilon_r(t)}{dt} \tag{16}$$

Similarly, the acceleration behind the test sample is calculated with the transmitted signal,

$$a_{t}(t) = \frac{dV_{t}(t)}{dt} = C_{0} \frac{d\varepsilon_{t}(t)}{dt}$$
(17)

In order to check the effect of wave dispersion, we applied an Endevco® 7270A-60K accelerometer at the transmission bar end (Fig. 1) to verify the acceleration calculated with the transmitted signal. We assume the addition of the accelerometer does not modify the wave propagation at the free end of the transmission bar,

$$a_{accel}(t) = 2a_{t}(t) = 2C_{0} \frac{d\varepsilon_{t}(t)}{dt}$$
(18)

It is noted that, due to stress wave dispersion from the strain-gage location to the bar end (accelerometer location), the time history of the accelerometer signal may be different from that of the acceleration calculated with a strain-gage signal, neither of which represents the actual acceleration right behind the foam specimen. In this case, it becomes more appropriate to compare the frequency spectra of accelerations measured with the accelerometer and calculated with the strain-gage signal (Eq. (18)),

$$a_{accel}(f) = FFT[a_{accel}(t)] = 2C_0 \cdot FFT \left[ \frac{d\varepsilon_t(t)}{dt} \right]$$
 (19)

In addition, the attenuation of acceleration through the foam sample can be calculated with the factor,  $\delta_a$ , calculated with the frequency spectra of incident, reflected, and transmitted accelerations as below,

$$\delta_{a}(f) = 1 - \frac{Mag[a_{t}(f)]}{Mag[a_{input}(f)]} = 1 - \frac{Mag[a_{t}(f)]}{Mag[a_{i}(f)] - Mag[a_{r}(f)]}$$
(20)

where Mag[a(f)] is the magnitude of Fourier transform (a(f)) of acceleration (a(t)) in the time domain. Equation (20) represents the frequency spectrum of acceleration attenuation through the foam sample.

#### **Experimental Results**

The PMDI foam investigated in this study had a density of  $0.32 \times 10^3$  kg/m³. The foam samples were made into 15.2-mm-diameter cylinders with three different thicknesses: 7.6 mm, 15.2 mm and 30.5 mm making the aspect ratios (L/Ds) of 0.5, 1 and 2, respectively. The maraging steel striker had a length of 152.4 mm, generating an approximate loading duration of 60  $\mu$ s. The foam samples were characterized at the same striker speed of 16 m/s. Additional tests at a higher impact speed (38 m/s) were also conducted on the 7.6-mm-thick foam sample.

Figure 2 shows a typical set of incident, reflected, and transmitted signals with a 7.6-mm-thick foam specimen. The striker speed was 16 m/s. Since the foam material possesses a very low strength, a pair of semiconductor strain gages was installed on the transmission bar to

measure the weak transmitted signal. The semiconductor strain gages had a gage factor of 155 which is approximately 75 times higher in sensitivity than regular resistance strain gages. As shown in Fig. 2, the amplitude of the transmitted strain is approximately 100 times lower than that of the incident strain. However, the semiconductor strain gages are capable of measuring a low-amplitude transmitted signal with a high resolution. In addition, the transmitted signal shows a much longer unloading portion in comparison to the incident and reflected pulses, because during dynamic unloading, the recovery force generated in the foam sample was too small to push the pressure bars back due to the weak strength particularly after the foam sample was damaged/cracked during impact loading. This makes the specimen unchanged in strain, but a decrease in stress occurs during the unloading stage, which can be interpreted as a "stress relaxation" response. This stress relaxation response allows the foam sample to release the stored energy. In this study, this portion of "stress-relaxation" energy was accounted for in the energy dissipation analysis, because the energy was eventually transmitted through the foam sample into the transmission bar. However, as shown in Fig. 2, the unloading portion of the transmitted pulse was so long as to be truncated (at  $t \approx 1600 \,\mu s$ ) by the reflected pulse at the free end, even though a 3650-mm-long transmission bar has been used in this study. We used the transmitted signal data right before it is truncated for energy dissipation analysis in this study. Figure 2 also shows the signal of the accelerometer that was attached to the free end of the transmission bar.

Fourier transform was applied to the incident, reflected, and transmitted signals. Equations (8)-(10) have then been used to calculate the spectral densities of energy associated with the incident, reflected, and transmitted pulses, respectively, the results of which are shown in Fig. 3. Figure 3 shows the impact energy is distributed in a frequency spectrum up to 60 kHz.

However, most incident energies over 10 kHz have been reflected back. Whereas, the transmitted energy has been concentrated into a very low frequency range up to 1.5 kHz. Figure 3 also shows the absolute dissipated energy decreases with increasing frequencies and then becomes nearly zero at the frequencies over 10 kHz due to the less input energy at such high frequencies. In order to investigate the energy dissipation characteristic through the foam sample, the energy dissipation ratio was calculated with Eq. (13) and plotted in Fig. 4. The energy dissipation ratio shown in Fig. 4 provides a clear frequency response characteristic in terms of energy dissipation. In fact, the impact energy was dissipated increasingly with increasing frequency. Nearly all impact energy with frequencies over 1.5 kHz has been absorbed by the foam material and not able to transmit through the foam material. The impact energy has been least absorbed at 0 Hz (DC), but there is still approximately 87% of total energy being absorbed at this frequency.

Figure 5 compares the frequency spectra of energy dissipation through the PMDI foam specimens with 1) different thicknesses at the same impact speed (~16 m/s); and 2) different impact speeds but with the same thickness (7.6-mm). The frequency spectra show very similar characteristic of energy dissipation. Particularly, all exhibit the same cutoff frequency at 1.5 kHz, above of which the energies are completely dissipated. When frequencies are below 1.5 kHz, the energy dissipation ratio decreases with decreasing frequencies. The energy dissipation ratio reaches the minimum value at 0 Hz (DC). The specimen thickness shows slight influence on the energy dissipation ratio when f < 1.5 kHz. At the same impact speed (16 m/s), the energy dissipation ratio for the 30.5-mm-thick specimen (87.8% at f = 0 kHz) is very close to that for the 7.6-mm-thick specimen (87% at f = 0 kHz), both of which are slightly higher than those for the 15.2-mm-thick specimens (82.5% and 85% at f = 0 kHz). Even for the exactly same conditions (same thickness of 15.2-mm and impact speed of 16 m/s), the results are slightly

scattered (82.5% versus 85.0% at f = 0 kHz), as shown in Fig. 5. This is probably due to the variation in cell structures of individual foam specimens.

With the same thickness (7.6-mm), the specimen subjected to a higher impact speed (38 m/s) exhibits a much higher energy dissipation ratio (96.3% at f = 0kHz) in comparison to 87% at the same frequency. This is because the higher impact speed subjected the specimen to a larger deformation, which allows the specimen to absorb more energy. Figure 6 shows the pictures of the foam specimens after the first loading at different impact speeds. At low impact speed (16 m/s), the foam specimen was deformed and no visible damage or crack was observed. However, at the higher impact speed (38 m/s), the foam specimen has been partially cracked, which absorbed more energy.

Figure 7 shows the comparison of acceleration histories through the 7.6-mm-thick specimen, measured at the bar free end with the accelerometer and calculated with the straingage signals (Eq. (18)), respectively. It is noted that the time zero (t = 0) has been reset as the time when the stress arrives at the specimen. As shown in Fig. 7, the differentiation of the straingage signal increases the high-frequency noise level. Therefore, a 500 kHz digital filter has been applied and the result is also plotted in Fig. 7. A difference was observed between the two measurements due to wave dispersion from the strain gage location to the free end of the bar. The frequency spectra of both time histories of the acceleration are plotted in Fig. 8(a), the results of which show more consistency. This demonstrates the appropriateness of frequency-domain analyses without the need of wave dispersion correction. Figures 8(b) and (c) show the frequency spectra of acceleration through the 15.2- and 30.5mm-thick specimens, respectively, at the same impact speed (16 m/s). All three specimens have the same cutoff frequency at approximately 125 kHz in terms of transmitted acceleration. Nearly no acceleration at the

frequencies over 125 kHz can be transmitted through the foam specimens, even the shortest (7.6-mm-thick) foam specimen. The dependency of the transmitted accelerations of the specimen thickness is insignificant. This is because the unique stress plateau in the compressive stress-strain response of the PMDI foam material. The same stress/force is transmitted through the specimen into the transmission bar before the specimen is densified, generating the same particle velocity and acceleration, independent of the specimen thickness. However, when the impact speed increases, the specimen may be densified, generating a higher transmitted force and subsequently a higher transmitted acceleration (shown in Fig. 9). Compared to the frequency spectrum shown in Fig. 8(a), it was observed that amplitudes did not significantly change when the frequencies are below 25 kHz, even though the time-domain transmitted acceleration was higher. With increasing impact speed, the spectrum was significantly changed at the frequencies higher than 25 kHz. Each frequency seems to exhibit the similar maximum value of amplitude, which may be related to the same duration of pulse according to Fourier transform theory.

Figure 10 shows the comparison of acceleration histories at both ends of the 7.6-mm-thick foam specimen. In the time domain, the input acceleration had a peak value of 200,000 g, which was attenuated to only 1500g (peak value) through the foam specimen. It is noted that the absolute value of acceleration attenuation is dependent on the material and dimensions of the transmission bar. For example, a transmission bar with a lower Young's modulus or a smaller cross section yields a higher transmitted acceleration for the same transmitted force. However, the acceleration attenuation factor calculated with Eq. (20) may represent the acceleration attenuation characteristic response to frequencies of the foam material. Figure 11 shows the frequency spectra of acceleration attenuation factors of the foam materials with different thicknesses and impact speeds. Since the attenuation approaches 1 when the frequencies are

higher than 3 kHz, only the acceleration attenuations at the frequencies lower than 5 kHz are shown in Fig. 11. Similar to the energy dissipation, the foam specimens exhibit the same cutoff frequency of approximately 1.5 kHz, showing little effect of specimen thickness. With increasing frequency, the attenuation factors increase and approach 1 at 1.5 kHz. With the same specimen thickness, the foam specimen subjected to a higher impact speed exhibits a similar attenuation factor at 0 Hz and then drastically approaches 1. Again, the characteristics of acceleration and its attenuation of the foam specimen are relevant to the experimental and specimen configurations, which can only be used for qualitative and relative comparison.

#### **Conclusions**

We employed the Kolsky compression bar technique to characterize the frequency response of shock mitigation, in terms of energy dissipation and acceleration attenuation, of a PMDI foam with different thicknesses and impact speeds. The time domain strain-gage measurements have been transformed into the frequency domain to calculate the sensitivities of impact energy dissipation and acceleration attenuation through the foam material to frequencies. The PMDI material investigated in this study exhibits superior shock mitigation capability for the frequencies over 1.5 kHz. Below 1.5 kHz, the shock mitigation decreases with decreasing frequencies. But even at 0 Hz (DC), the PMDI foam material still dissipates impact energy and attenuates acceleration in a very good manner. The shock mitigation capability of the PMDI foam seems insignificantly dependent on the specimen thicknesses but is notably affected by impact speed. The experimental and analytical methods presented in this study can be applied to

any other materials for shock mitigation assessment and will help for material design, selection, and optimization in shock mitigation applications.

# Acknowledgements

The authors would like to thank Dr. Wei-Yang Lu for providing the foam materials and Terry Hinnerichs and David Lo for technical discussions. The authors also thank Dr. Edmundo Corona and Thomas Bosiljevac for their valuable comments on this manuscript.

Sandia National Laboratories is a multi-program laboratory managed and operated by Sandia Corporation, a wholly owned subsidiary of Lockheed Martin Corporation, for the U.S. Department of Energy's National Nuclear Security Administration under contract DE-AC04-94AL85000.

#### References

- [1] Gibson, L.J., and Ashby, M.F., 1999, Cellular solids, structure and properties, 2<sup>nd</sup> edn. Cambridge University Press, Cambridge
- [2] Ashe, W.A., 1988, Rigid cellular plastics in automotive applications, ASTM Standard News, 16: 32-33
- [3] Weiser, E.S., Johnson, T. F., Clair T.L.S., Echigo, Y., Kaneshiro, H., and Grimsley, B.W., 2000, Polyimide foams for aerospace vehicles, High Performance Polymers, 12:1-12
- [4] Mills, N.J., and Gilchrist, A., 2008, "Oblique impact testing of bicycle helmets," International Journal of Impact Engineering, 35:1075-1086
- [5] DeMarco, A.L., Chimich, D.D., Gardiner, J.C., Nightingale, R.W., and Siegmund, G.P., 2010, "The impact response of motocycle helmets at different impact severities," Accident Analysis and Prevention, 42:1778-1784
- [6] Landro, L.D., Sala, G., and Olivieri, D., 2001, "Deformation mechanisms and energy absorption of polystyrene foams for protective helmets," Polymer Testing, 21:217-228
- [7] Song, B., Chen, W., Dou, S., Winfree, N.A., and Kang, J.H., 2005, "Strain-rate effects on elastic and early cell-collapse responses of a polystryrene foam," International Journal of Impact Engineering, 31:509-521
- [8] Throne, J.L., 1985, "Effect of density on compressive stress-strain behavior of uniform density closed cell foams," Journal of Cellular Plastics, 21:178-182

- [9] Chen, W., Lu, F., and Winfree, N.A., 2002, "High-strain-rate compressive behavior of a rigid polyurethane foam with various densities," Experimental Mechanics, 42:65-73.
- [10] Song, B., Chen, W., Yanagita, T., and Frew, D.J., 2005, "Confinement effects on the dynamic compressive properties of an epoxy syntactic foam," Composite Structures, 67:279-287
- [11] Song, B., Chen, W., Yanagita, T., and Frew, D.J., 2005, "Temperature effects on dynamic compressive behavior of an epoxy syntactic foam," Composite Structures, 67:289-298
- [12] Song, B., Lu, W.-Y., Syn, C.J., and Chen, W., 2009, "The effects of strain rate, density, and temperature on the mechanical properties of polymethylene diisocyanate (PMDI)-based rigid polyurethane foams during compression," Journal of Material Sciences, 44:351-357
- [13] Bateman, V.I., Brown, F.A., and Hoke, D.A., 2001, Structural foam characteristics in a mechanical shock environement, Sandia report, SAND2001-2674
- [14] Song, B., and Chen, W., 2006, "Energy for specimen deformation in a split Hopkinson pressure bar experiment," Experimental Mechanics, 46:407-410
- [15] Beccu, R., and Lundberg, B., 1987, "Transmission and dissipation of stress wave energy at a percussive drill rod joint," International Journal of Impact Engineering, 6:157-173
- [16] Kolsky, H., 1963, Stress Waves in Solids, Dover, New York
- [17] Follansbee, P.S., and Frantz, C., 1983, "Wave propagation in the split Hopkinson pressure bar," Transactions of the ASME, Journal of Engineering Materials and Technology, 105:61-66
- [18] Werner, B.T., Song, B., and Nelson, K., 2014, "Effect of threaded joint preparation on impact energy dissipation using frequency-based Kolsky bar analysis," In: Proceedings of 2014

SEM Annual Conference and Exposition on Experimental and Applied Mechanics, June 2-5, 2014, Greenville, SC, USA.

### **Captions of Figures**

- Figure 1. Schematic of Kolsky compression bar for foam testing
- Figure 2. Oscilloscope records in a Kolsky compression bar test of a 7.6-mm-thick PMDI foam specimen
- Figure 3. Frequency spectra of energy densities associated with incident, reflected, and transmitted waves as well as energy dissipation
- Figure 4. Energy dissipation ratio in frequency domain
- Figure 5. Frequency-domain energy dissipation ratios with different specimen thicknesses and impact speeds
- Figure 6. Pictures of specimens before and after dynamic testing with different impact speeds
- Figure 7. Comparison of free-end accelerations
- Figure 8. Frequency spectra of free-end accelerations at the same impact speed (16 m/s). a) 7.6-mm-thick specimen; b) 15.2-mm-thick specimen; c) 30.5-mm-thick specimen
- Figure 9. Frequency spectra of free-end accelerations at 38 m/s
- Figure 10. Input and transmitted accelerations through a 7.6-mm-thick foam specimen
- Figure 11. Acceleration attenuation though different-thickness specimens at different impact speeds.

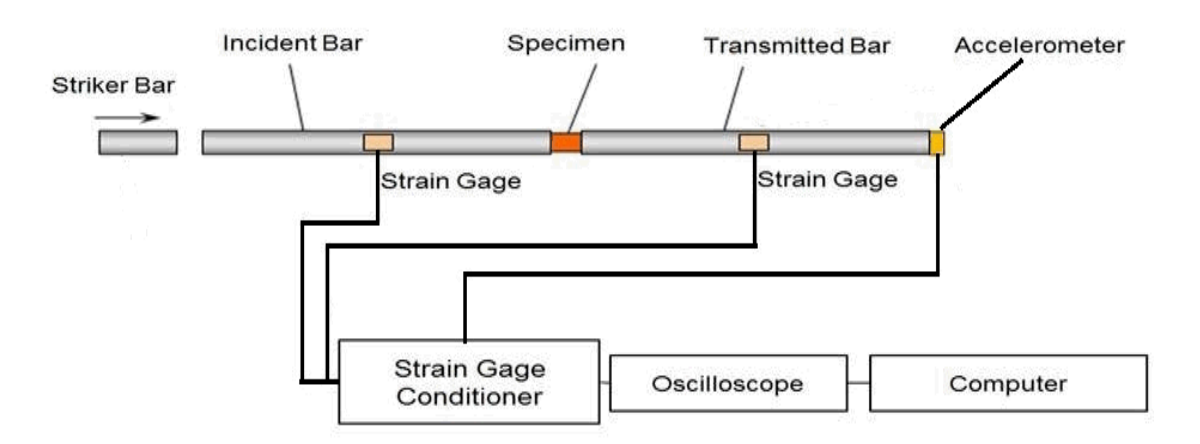


Figure 1

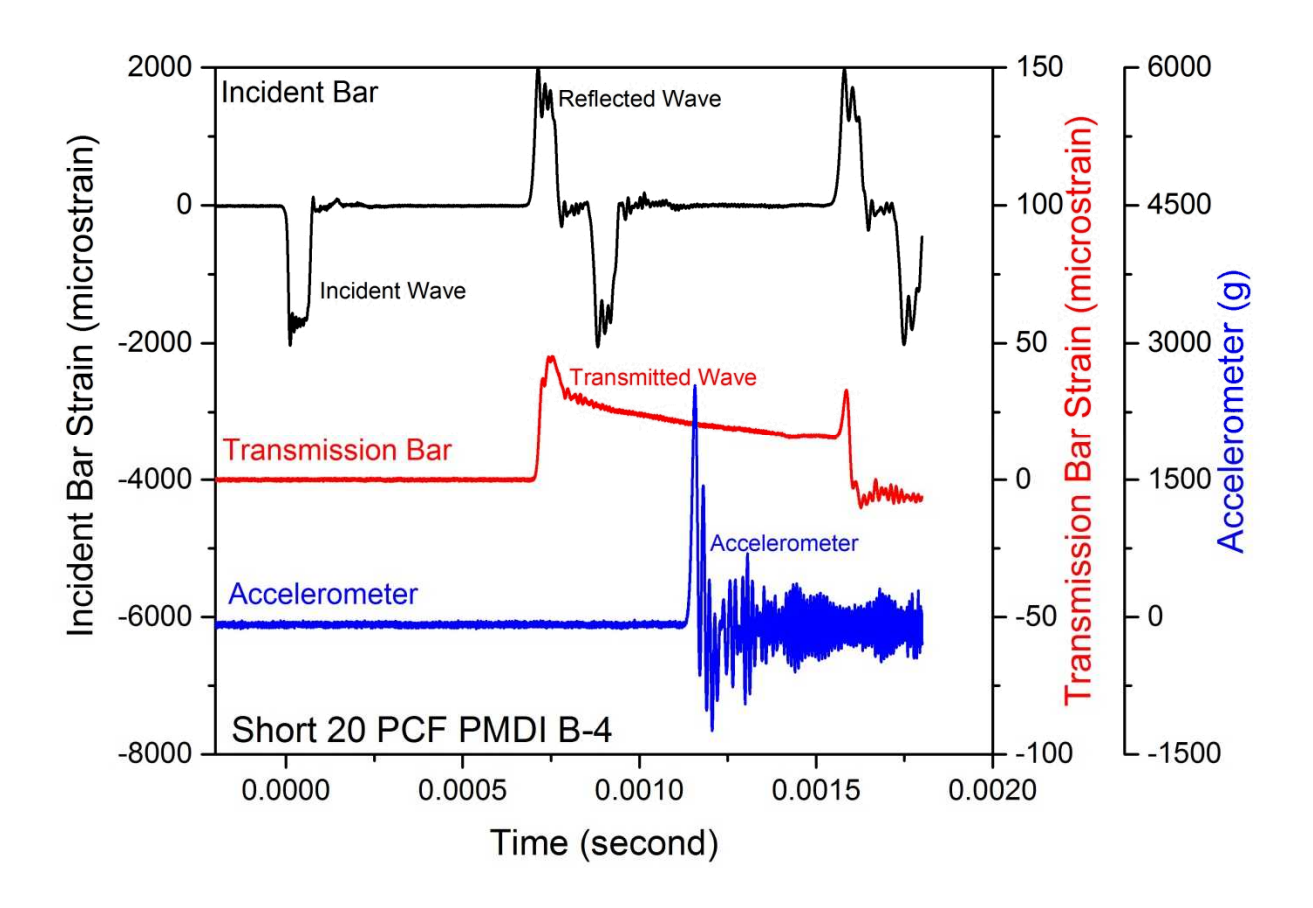


Figure 2

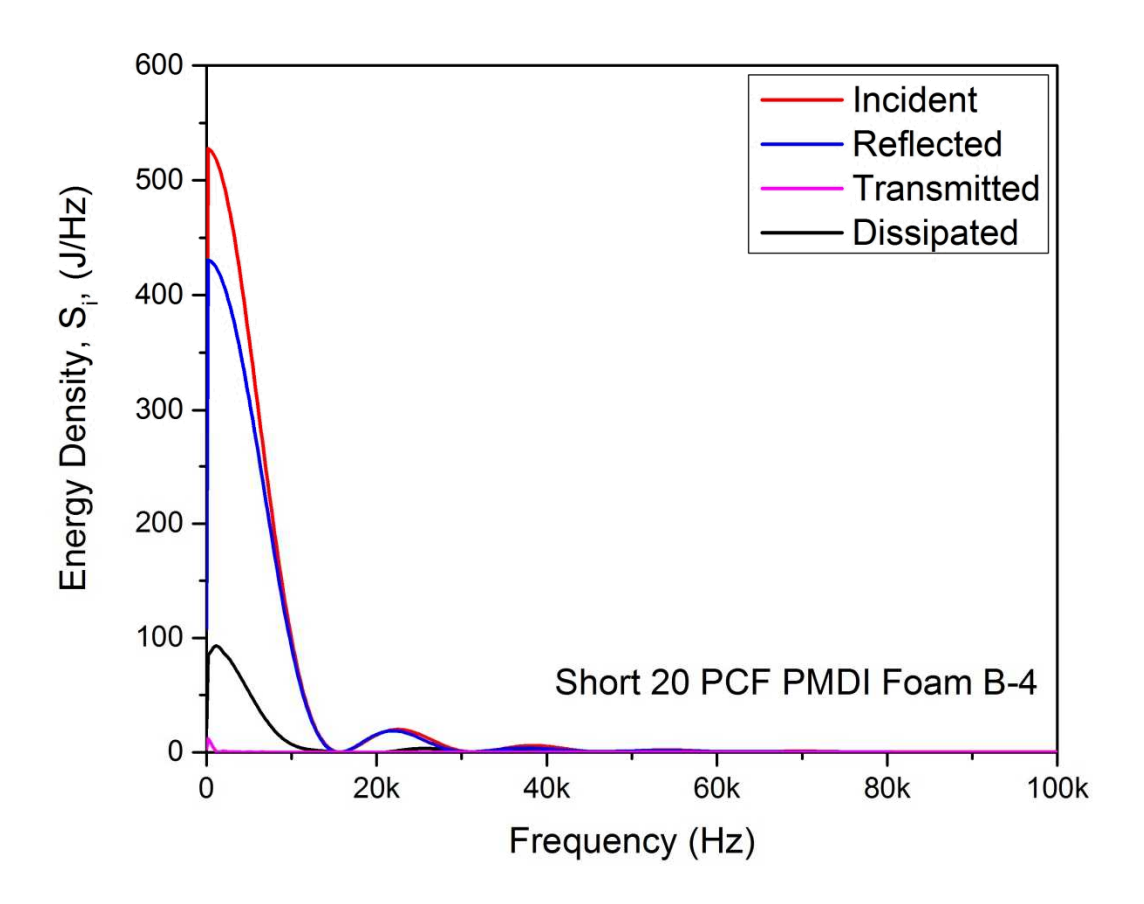


Figure 3

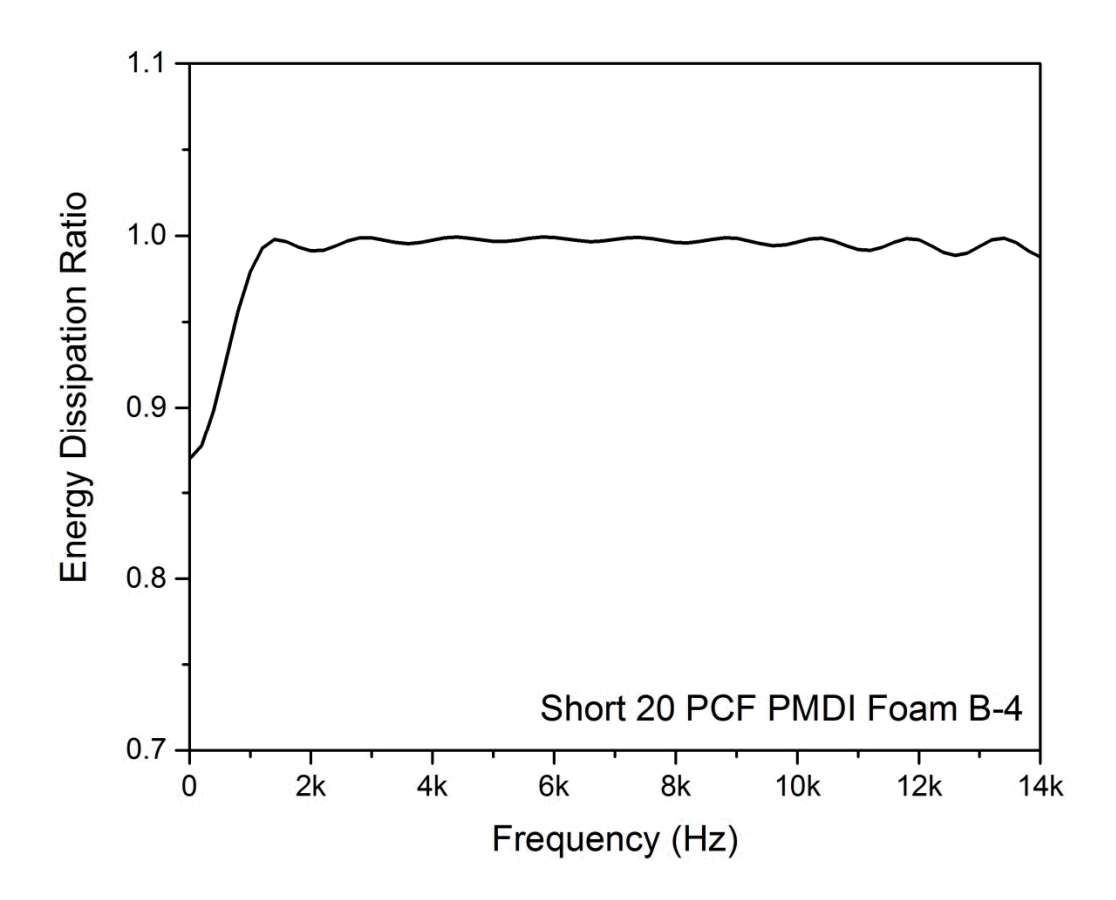


Figure 4

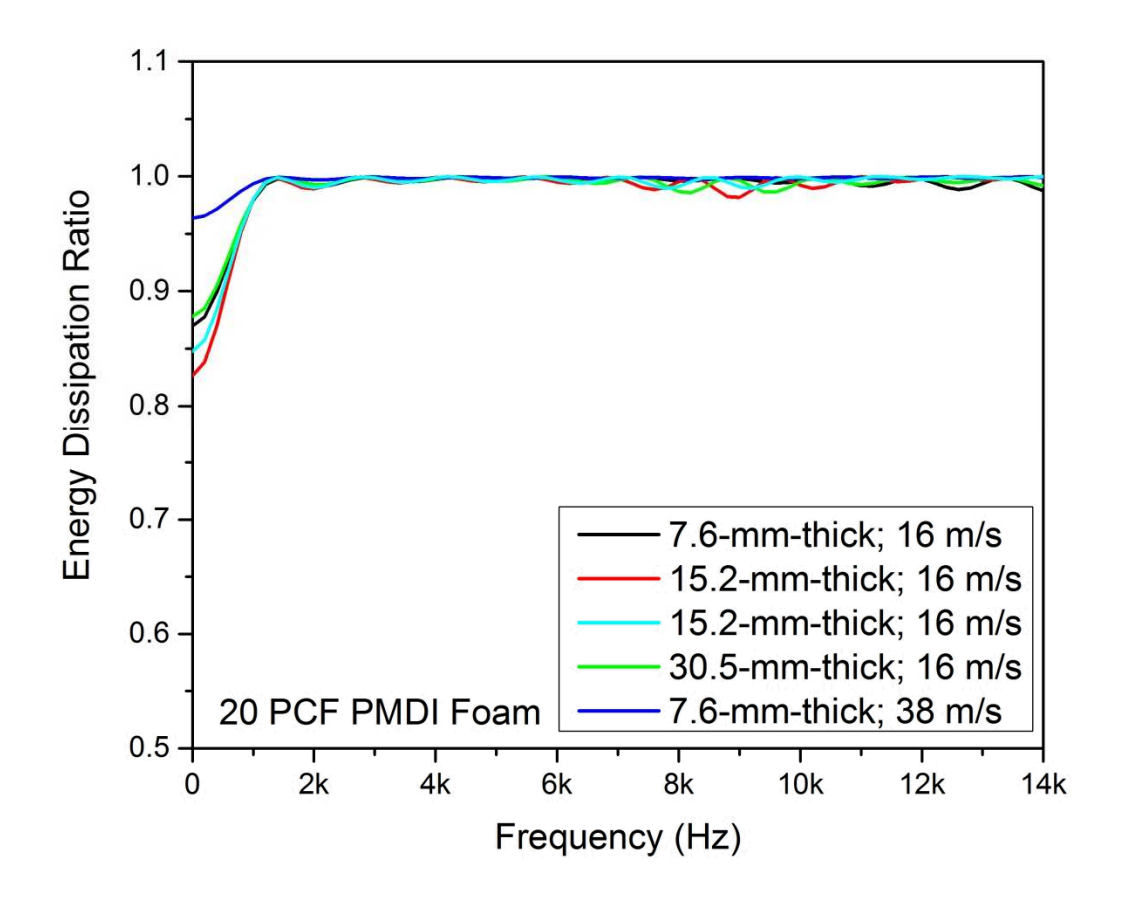


Figure 5



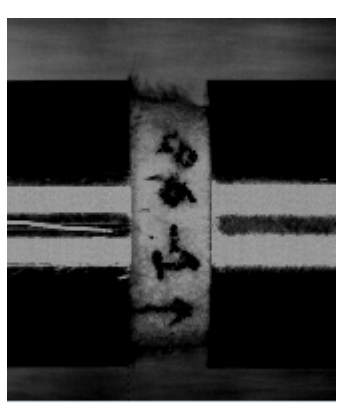


Before

After First Loading

(a) V=16 m/s





Before

After First Loading

(b) V=38 m/s

Figure 6

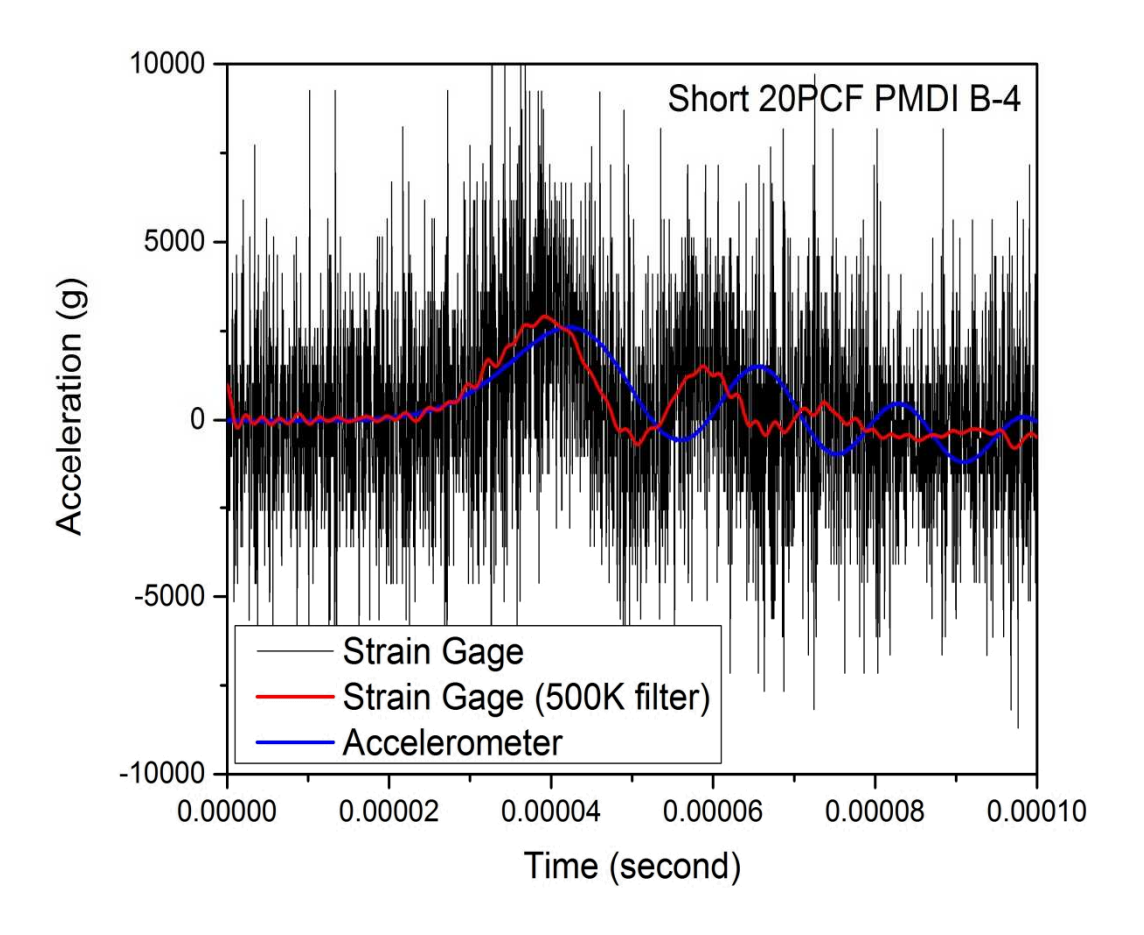
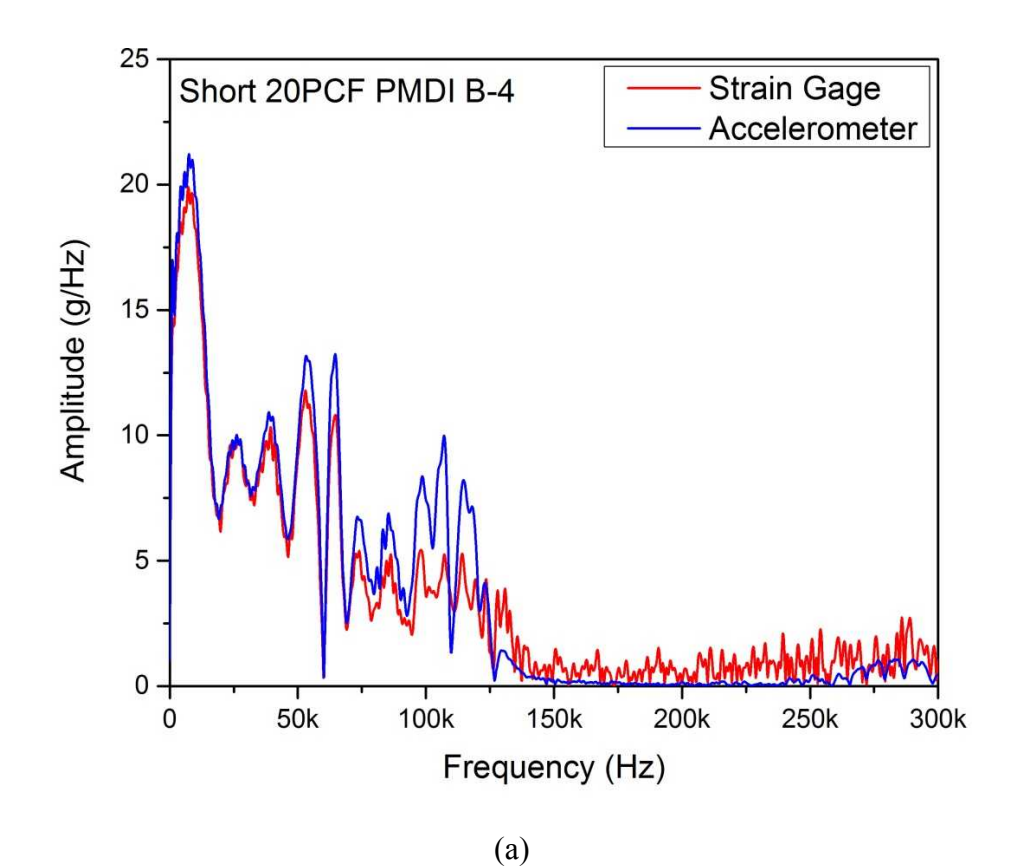


Figure 7



25 Medium 20PCF PMDI A-3 Strain Gage Accelerometer 20 Amplitude (g/Hz) 15 10 5 0 0 50k 100k 150k 200k 250k 300k Frequency (Hz)

(b)

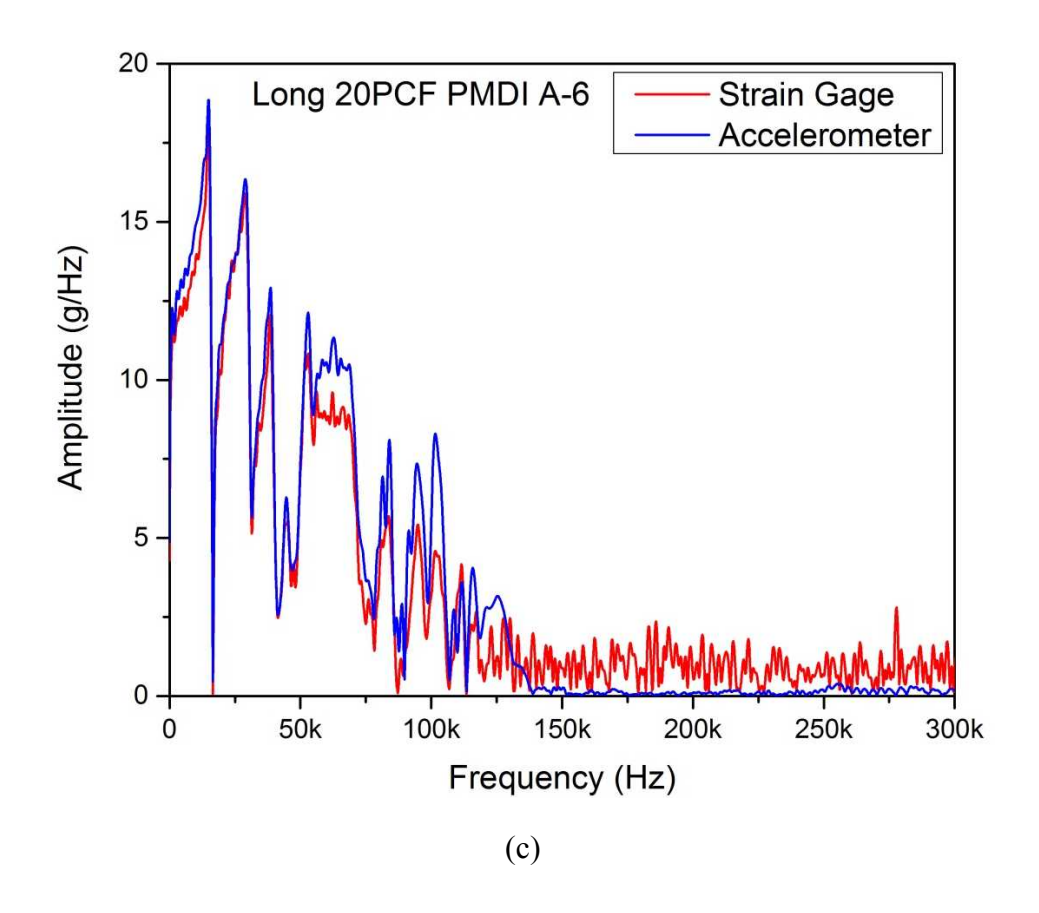


Figure 8

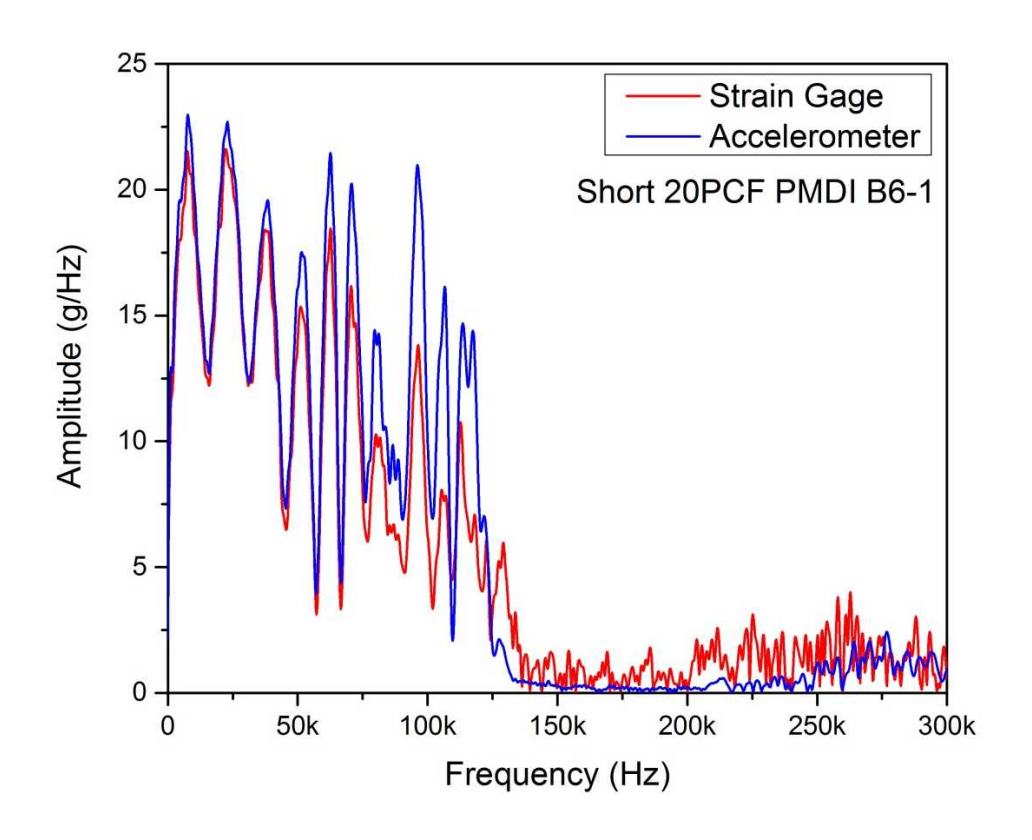


Figure 9

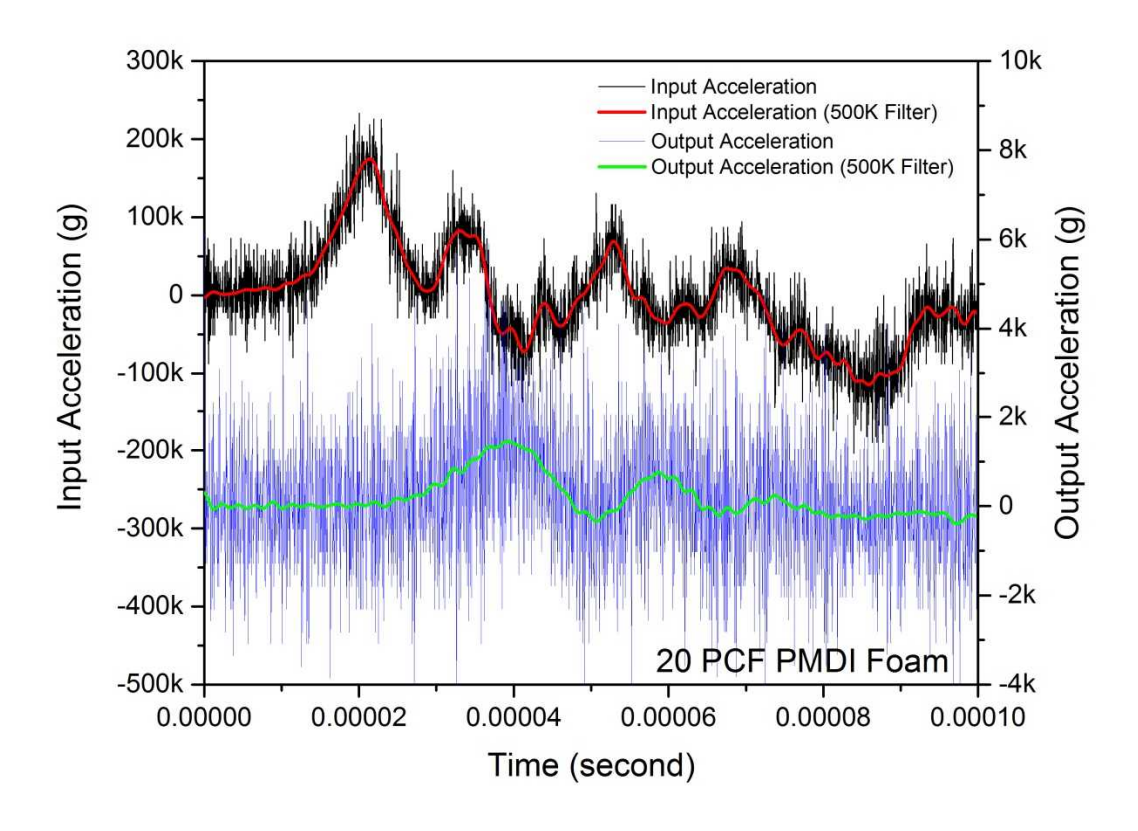


Figure 10

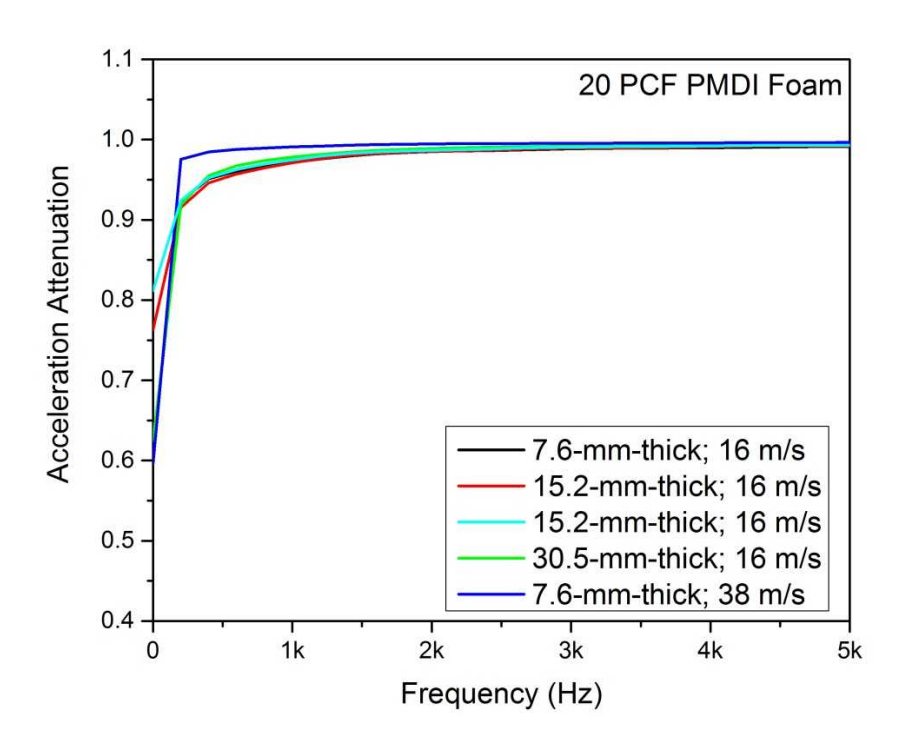


Figure 11